Journal of Hydrology (2008) **361**, 10–23

available at www.sciencedirect.com

ScienceDirect

journal homepage: www.elsevier.com/locate/jhydrol

Using meteorological data to forecast seasonal runoff on the River Jhelum, Pakistan

D.R. Archer [a,*], H.J. Fowler [b]

[a] *JBA Consulting, South Barn, Broughton Hall, Skipton, North Yorks, England BD23 3AE, United Kingdom*
[b] *Water Resource Systems Research Laboratory, School of Civil Engineering and Geosciences, Newcastle University, United Kingdom*

Received 12 October 2007; received in revised form 24 June 2008; accepted 17 July 2008

KEYWORDS
River Jhelum;
Seasonal flow forecasting;
Summer runoff;
Multiple linear regression;
Water management

Summary The upper River Jhelum, which drains the southern slopes of the Himalaya and Pir Panjal, provides water for power and irrigated agriculture, the mainstay of the national economy of Pakistan. Seasonal forecasts of spring and summer flow provide the opportunity for planning and would confer significant national benefits.

In this mountainous region, runoff from snowmelt and glacier-melt provides the dominant contribution to river flows during the spring and summer seasons although monsoon rainfall may also influence peak flows. Estimates of runoff in the Jhelum and its main tributaries can be made using precipitation measurements from valley stations; producing correlation coefficients of >0.7 between winter precipitation and spring and summer runoff.

This study investigates the links between climate and runoff for eight gauging stations in the Jhelum catchment but then concentrates on seasonal forecasting of spring and summer inflows to Mangla Dam which is a major controlling structure contributing to the Indus Basin Irrigation System. Observed climatic variables, precipitation and temperature, from valley stations are used to forecast summer season flows at stations upstream from the reservoir with a lead time of up to three months based on multiple linear regression models built using data from 1965 to 1979. The analysis demonstrates that good forecasts within 15% of observed flows for 92% of years (ROC score = 0.77) can be achieved for summer season flows from April to September over the 1980–1991 validation period. For spring flows from April to June, excellent forecasts can be provided within 15% of observed flows for 83% of years, with a ROC score of 0.93. These provide a useful basis for practical water management.

* Corresponding author. Address: 2 Welburn Close, Ovingham, Northumberland NE42 6BD, United Kingdom. Tel.: +44 1661 834063.
E-mail addresses: david.archer@jbaconsulting.co.uk (D.R. Archer), h.j.fowler@ncl.ac.uk (H.J. Fowler).

0022-1694/$ - see front matter © 2008 Elsevier B.V. All rights reserved.
doi:10.1016/j.jhydrol.2008.07.017

Introduction

The River Jhelum and its principal tributaries, the Neelum and Kunhar, drain the southern slopes of the Himalaya and parts of the Pir Panjal Range (Fig. 1) in Jammu and Kashmir. The catchment is divided by the Line of Control between India and Pakistan. The Jhelum then flows through the plains of the Punjab, where there are significant agricultural water deficits, before joining with the Sutlej, Beas, Ravi and Chenab and finally with the Indus at Mithankot. Although monsoon rainfall affects the lower part of the catchment, runoff from the melting of winter snow and perennial ice makes a significant contribution to river flow during the summer season; vital for irrigation and hydropower production in the region.

Until 1967 the irrigation system of Pakistan was dependent on the natural flow regime of the Indus and its major tributaries. However, the construction of two major reservoirs, Mangla Dam on the Jhelum River in 1967 and Tarbela on the Indus commissioned in 1976, with fifteen downstream barrages and a network of canals and distribution channels has transformed the management of irrigated agriculture in the region. The Indus Basin Irrigation System serves an area of 14 million hectares and irrigated land accounts for 85% of all cereal grain production (mainly rice and wheat), all sugar production and most cotton production (Khan et al., 2002). The command area of Mangla is 6 million ha. More effective irrigation management could be achieved by improved management of the major storage reservoirs and, particularly, by improved forecasting of seasonal inflows.

A significant secondary function of Mangla is the generation of electric power. Mangla has an installed capacity of 1000 MW which is 6% of the total installed capacity of all sources for Pakistan (Asianics Ltd, 2000). Since irrigation demand has the first priority on water released from Tarbela, the production of energy occurs either as a by-product of irrigation releases or when surplus water to irrigation needs is available. Seasonal flow forecasting could provide significant benefits for the management of national power strategies by providing an early indication of surplus or shortfall in hydropower which would require balancing with thermal power sources.

Data

River gauging stations at locations in the Jhelum basin used in this analysis are shown in Fig. 1, and station information is shown in Table 1. Streamflow measurement in Pakistan is carried out by the Water and Power Development Authority—Surface Water Hydrology Project (WAPDA—SWHP). An outline of the methods of streamflow measurement and an assessment of the quality of records is provided in Archer (2003). The available flow record for Mangla since reservoir construction is an outflow record and is therefore partly dependent on reservoir operating policy as well as natural inflow. Reliance for assessment of inflow has therefore been primarily based on upstream flow records.

WAPDA also maintain a network of climatological stations, but most of the climatological records used in this analysis were obtained from the Pakistan Meteorological Department. Most stations have records in excess of 30 years, commencing around 1960, but a much longer record from 1893 for Srinagar was obtained from the Climate Research Unit at the University of East Anglia, England. A total of fourteen stations (Table 1) within the catchment and on its margins have been examined.

Environmental conditions in the Jhelum basin

The Jhelum rises on the north-western side of Pir Panjal and receives tributaries from the southern slopes of the Greater Himalaya which are fed in part by glaciers and partly by the melting of seasonal snow (Fig. 1). It drains alluvial lands in the Kashmir Valley and flows through the large Wular Lake which significantly attenuates the seasonal flood wave. On emergence from the Wular Lake, it runs through a 130 km long gorge before being joined near Muzafferabad by its largest tributary the Neelum (also called the Kishan Ganga) and 8 km downstream by the Kunhar. Two further important tributaries join in the lower reaches, the Kanshi and the Poonch, which flow directly into Mangla Reservoir. The Kanshi drains eroded lowland areas to the east of the reservoir, whilst the Poonch rises on the southern slopes of the Pir Panjal range.

Annual rainfall varies from 683 mm at Srinagar in the upper Jhelum catchment to over 1600 mm at Garhi Dupatta, then declining southward to 873 mm at Mangla (Table 1). Over the period from 1961 to 1990 annual rainfall totals have typically ranged from 70% of the mean to a maximum of 135% of the mean.

Two distinct seasonal rainfall regimes occur in the Jhelum basin. In the south there is a bimodal rainfall distribution with peaks in spring centred on March and a greater peak during the summer monsoon centred on July and with minima in May and November (Fig. 2a). Typically, over 700 mm occurs during the four months from June to September; representing about 50% of the annual total. The seasonal total decreases southward but the proportion of the annual total increases to 66% at Mangla. The spring peak, by comparison, represents around 30% of the annual total, decreasing southward.

In contrast, in the northern and eastern part of the basin there is a single peak in spring (Naran) or the summer peak is weakly developed (Srinagar) (Fig. 2b). Over 50% of annual precipitation occurs in the January to April period for both stations but only 16% in the monsoon period at Naran and 29% at Srinagar. Although the number of currently available stations in the upper part of the catchment is limited, the seasonal distribution for the high mountain areas of the Himalaya is supported by the record at Astore in a neighbouring catchment. In addition, pre-Partition records for Gurais in the Upper Neelum catchment and Baramula in the Vale of Kashmir also show a strong spring maximum. Winter precipitation for the whole catchment is positively related to elevation and, as measurement stations are located in valleys, it is postulated that catchment precipitation is significantly greater than the available measurements. Hewitt (2005) indicates that the elevation at which maximum precipitation occurs in the neighbouring Karakoram is between 5000 and 6000 m.

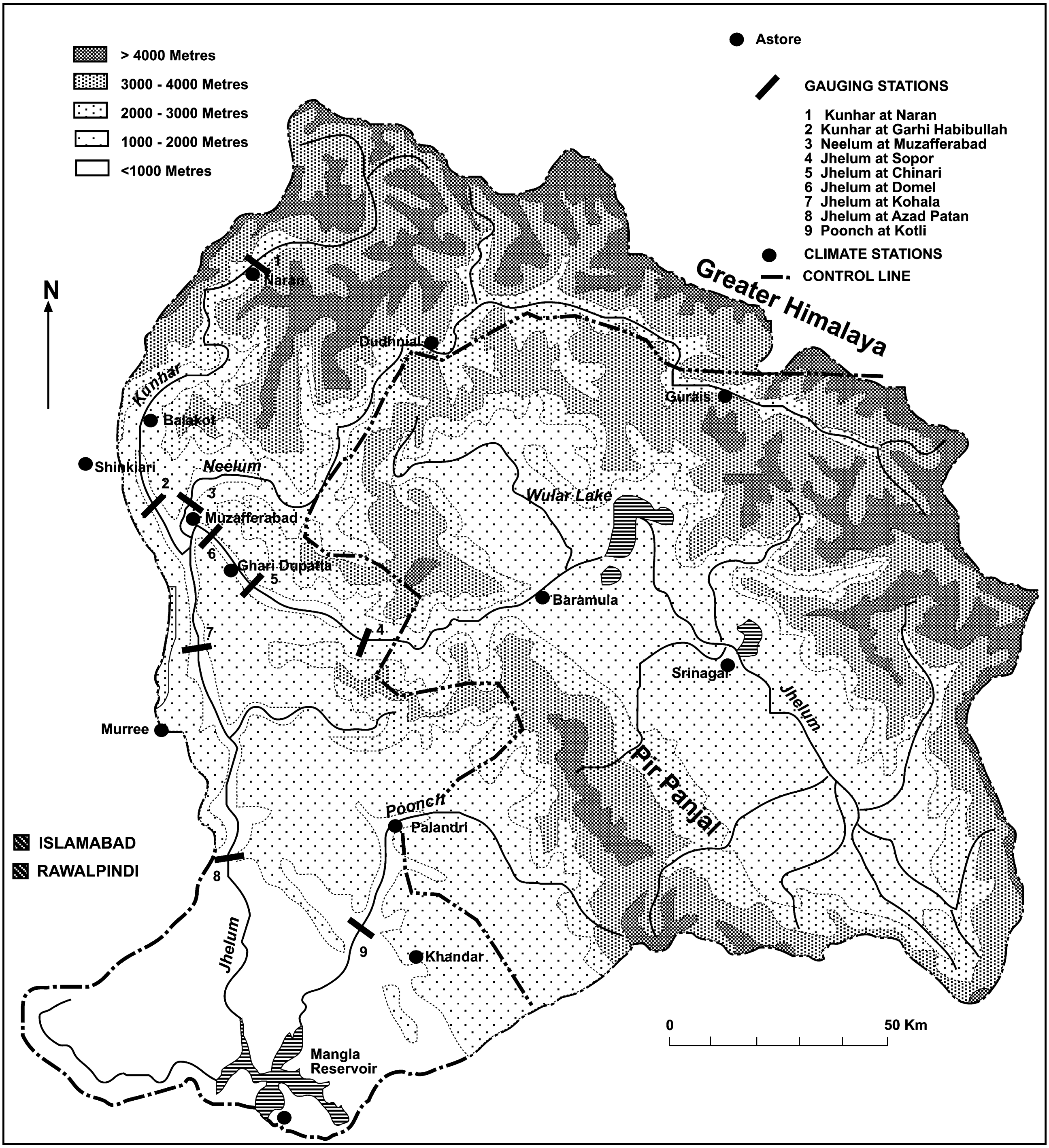

Figure 1 The Jhelum Basin showing relief and the river flow and climate stations used in this analysis.

There appears to be a distinct dividing line between the two regimes at the Pir Panjal Range which restricts the northward penetration of the summer monsoon. However, Archer and Fowler (2004) have shown that winter and spring precipitation, by contrast, is strongly correlated on both sides of the Himalayan divide, resulting from westerly disturbances.

Annual runoff is between 750 and 850 mm for the Jhelum above the Neelum confluence, 1500—1700 mm for the Neelum, and 1125 mm for the Kunhar (Table 1). Annual runoff at Mangla is 856 mm. The annual percentage contribution of the three tributaries to the total flow below their confluence is 45%, 43% and 12% for the Jhelum, Neelum and Kunhar, respectively. The Jhelum produces a greater proportion during the winter and spring, reaching 65% of the total in March. The Neelum and Kunhar contribute a greater proportion in summer — respectively 53% and 14% in July.

Spring rise in water level (Fig. 3) is earlier than on most Upper Indus tributaries, and earlier on the Jhelum than on the Neelum and Kunhar. Peak mean monthly flow is in May

Table 1 Station location and catchment information for (a) gauging stations and (b) climate stations, in and adjacent to the Jhelum basin

River	Station	Period of available record	Basin area (km^2)	Mean elevation (m)	Mean flow (m^3/s)	Annual runoff or rainfall (mm)
Flow gauging stations						
Jhelum	Sopor	1963–1988	c. 9000		229	801
Jhelum	Chinari	1970–1994	13775	2437	330	756
Jhelum	Domel	1976–1996	14375	2402	374	821
Neelum	Dudhnial		4905	3512	266	1710
Neelum	Nosheri	1991–1996	6807	3320	365	1692
Neelum	Muzafferabad	1963–1996	7392	3215	357	1524
Kunhar	Naran	1960–1998	1895	3512	48	799
Kunhar	Garhi Habibullah	1960–1990	2855	3215	102	1129
Jhelum	Kohala	1965–1996	25000	2629	828	1045
Jhelum	Azad Patan	1978–1996	26675	2545	910	1075
Kanshi	Palote	1970–1996	1172	520	7	183
Poonch	Kotli	1960–1996	3176	1805	134	1333
Jhelum	Mangla	1922–2000	33342		905	856
Climate stations						
	Srinagar	1893–1999		1587		683
	Astore	1954–1997		2394		517
	Naran	1961–1996		2363		1221
	Dudhnial	1993–1995		1816		1286
	Balakot	1961–1990		980		1671
	Shinkiari	1961–1996		991		1344
	Muzafferabad	1962–1992		686		1367
	Domel	1962–1992		686		1396
	G.Dupatta	1955–1992		813		1623
	Murree	1960–1991		2206		1804
	Rawalakot	1960–1992		1677		1383
	Palandri	1962–1992		1402		1450
	Khandar (Nakial)	1961–1992		1067		1264
	Mangla	1960–1992		282		862

for the Jhelum, June for the Neelum and lower Kunhar but July for the upper Kunhar at Naran. The peak for southern tributaries, Kanshi and Poonch, is in August but influenced by extreme outlier high flows in that month. A broad peak at Mangla is equally divided between June and July.

The seasonal percentage of runoff from April to June is higher than for July to September on all three tributaries although the Neelum has only marginally greater flows in spring at Muzafferabad. The upper Kunhar at Naran has higher summer runoff. The Kanshi and Poonch have quite different seasonal patterns from the other tributaries with a much higher summer percentage derived from monsoon rainfall rather than snowmelt and a significant proportion in winter (both) and spring (Poonch) derived from direct winter rainfall and early melt of snow at lower elevations.

The rationale for seasonal forecasting

Forecasting of seasonal runoff volume from the melting of accumulated snow is a long-established practice in many basins in North America, Europe and Russia (Quick, 1972; Popov, 1972). Such forecasts depend primarily on observation of snowpack water content obtained by snow course surveys and by snow pillow observations (Farnes, 1985), although early use was also made of rainfall measured at valley stations as an index of basin precipitation (Garstka, 1964). Airborne (Carroll, 1995) and satellite remote sensing data (Hall and Martinec, 1985) now provide supplementary information on snow cover area and properties. It has also been shown by Schär et al. (2004) that model-assimilated precipitation data provide an effective means of seasonal runoff forecasting. Precipitation from the 15-year Re-Analysis (ERA-15) (Gibson et al, 1999) has been used effectively for prediction on the Syrdarya basin in Central Asia.

Early forecasting practice relied on the derivation of regression relationships between seasonal runoff and snow cover (Quick, 1972). More recently, wider use has been made of simulation, using appropriate physically-based models (Day, 1985). Additionally, seasonal forecasts of climatological variables are now issued routinely by a number of meteorological centres (Wedgbrow et al., 2002) allowing increasing consideration to be given to the impact of large-scale oceanic-atmospheric variability (Wood et al., 2002;

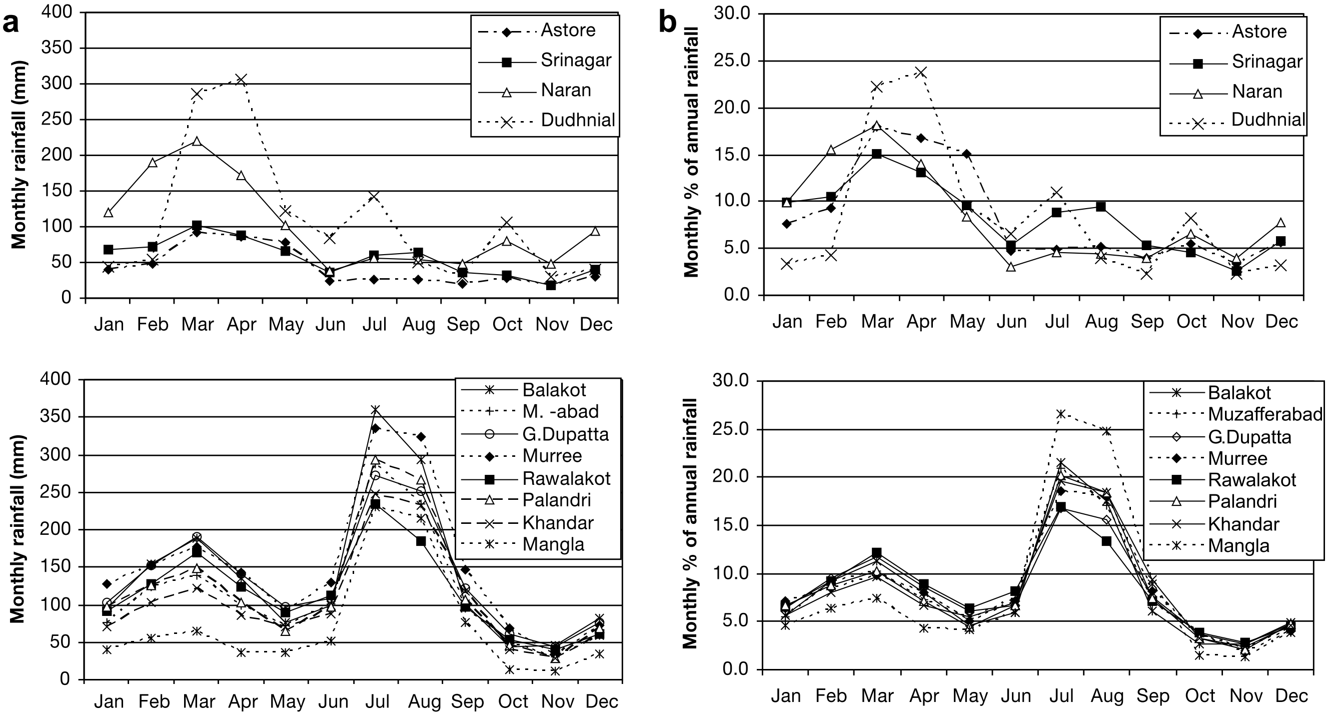

Figure 2 Monthly rainfall stations for: (a) stations in the north and east of the Jhelum basin, and (b) stations in the south of the Jhelum basin. Left panels show monthly rainfall (in mm) and right panels show monthly rainfall as a percentage of annual rainfall.

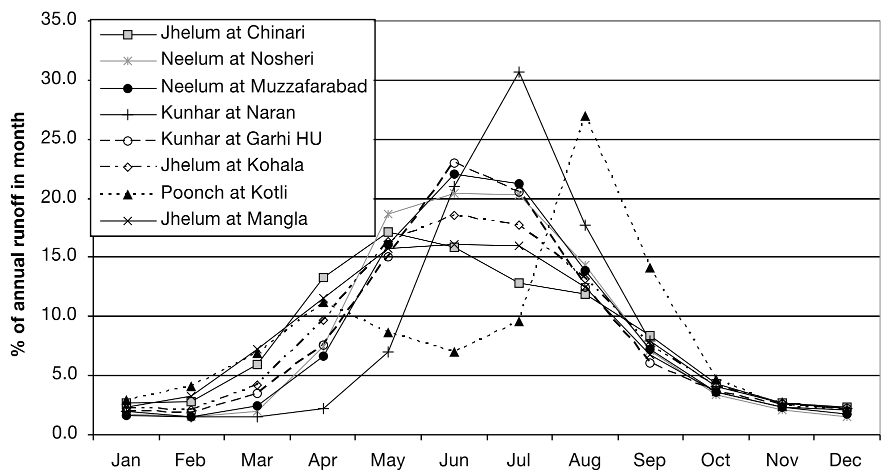

Figure 3 Distribution of mean monthly flows (as a percentage of annual) for gauged stations in the Jhelum basin (see Fig. 1 for location of gauges).

Clark et al., 2003). Indeed, a number of remote forcing sources of climate variability have been identified for Central and Southwest Asia. These include the El Niño Southern Oscillation (ENSO, e.g., Mason and Goddard, 2001; Mariotti et al., 2005), the North Atlantic Oscillation (NAO, e.g., Archer and Fowler, 2004; Syed et al., 2006), the combination of ENSO conditions and western Pacific SSTs (Barlow et al., 2002; Hoerling and Kumar, 2003), the Indo-Pacific Warm Pool region (Barlow et al., 2002, 2005), as well as the large-scale temperature response to the intensity of the South Asian monsoon (e.g., Rodwell and Hoskins, 1996; Schiemann et al., 2007).

Seasonal runoff forecasting in the Himalaya and neighbouring mountains is, by contrast, still at an early stage. The rugged terrain is a serious obstacle to ground-based observation of snow cover at high elevation, although strong correlation between annual snowpack water equivalent and runoff has previously been found in the Kunhar tributary of the Jhelum (De Scally, 1994). Satellite observation of the areal extent and depletion of the snowpack has been used in the Upper Indus Basin (UIB) (Rango et al., 1977; Dey et al., 1983) as a basis for assessing snowpack water equivalent and runoff. However, relationships in the UIB were calibrated with very short observed records and subsequent application has proven unreliable (Makhdoom and Solomon, 1986).

Although there is potential for the further development of forecasting based on satellite observation, hydrological research in the UIB (Kolb, 1992; Archer, 2003, 2004; Archer and Fowler, 2004; Fowler et al., 2005; Fowler and Archer, 2006) indicates that climatological measurements at valley stations may be valuable in the forecasting of seasonal runoff. Strong spatial correlation in winter (October—March) precipitation occurs across the UIB, so that winter snow accumulation can be indexed by rainfall measured at valley level. Such ground-based data have the distinct advantage of a long period of historic (and continuing) record with which to calibrate and verify relationships and have also been found to be valuable elsewhere in central Asia (Schär et al., 2004).

Archer (2003) established that in the Upper Indus there are strong links between seasonal climate and summer (July—September) runoff. However, the climatic variables which control runoff differ between sub-catchments depending on whether they are fed primarily by glaciers and permanent snow packs, by the melting of seasonal snow, or by rainfall. Highly glaciated catchments such as the Rivers Hunza and Shyok in the Karakoram Mountains have high correlation coefficients between summer temperature (June—September) and concurrent summer runoff and show non-significant links between winter precipitation and summer runoff. In contrast, catchments fed by the melt of seasonal snow, such as that part of the River Astore and Upper Indus draining areas adjacent to the Jhelum, show strong links between winter (October—March) precipitation and summer runoff (June—September).

For the Upper Indus, runoff arising from incident rainfall during the summer is very limited. Although occasional monsoon incursions with intense rainfall occur in trans-Himalayan areas, these usually result in declining river flows as they are accompanied by lowered temperatures and reduced energy inputs to the snowpack (Archer, 2004), with the closing down of ablation at higher elevations more than compensating for the direct rainfall contribution to runoff at lower elevations.

The same principles of linear regression and correlation have been applied to the Jhelum but recognising the relatively increased spring compared to summer runoff, and the increased contribution of monsoon rainfall (Binnie and Mansell-Moulin, 1966; Binnie et al, 1967). Discharge ($m^3\,s^{-1}$) has been preferred to runoff (mm) since discharges from catchments of different sizes can be summed, but not runoff. Correlation coefficients as shown in Tables 2 and 3 are numerically equivalent for discharge and runoff.

This paper first considers climate-runoff links at a number of gauging stations in the Jhelum basin but then concentrates on seasonal forecasting of inflow to Mangla Dam based on upstream stations on the main stem of the Jhelum at Kohala and the River Poonch at Kotli. Whilst the current management of releases from Mangla incorporates short-term flow forecasting predominantly provided for a 10-day period, there is no current system for forecasting flows for periods in advance of one month. Therefore, the outputs from this study could provide a practical method for the longer term forecasting of summer flows.

Climate runoff links for Jhelum gauging stations

The strengths of linkages between seasonal climate and streamflow parameters and how these vary through the Jhelum basin have been examined using seasonal correlations between rainfall and flow for long period gauging stations and precipitation records at Astore, Srinagar, Muzafferabad, Balakot and Murree (Table 2). Seasonal correlations between flow and mean seasonal temperature at Astore, Srinagar and Murree were also established (Table 3). Key results are summarised for flow periods April—June, April—September and July—September. For each flow station, the rainfall station with the highest correlation coefficient (*r*) is noted in the first line and the best correlation coefficient in line 2. The Mangla record has been broken into two parts, the early record from 1922 to 1959 for which only concurrent climate data for Srinagar were available, and the later reservoir outflow record following dam construction. For the latter only the relationship for the whole spring and summer season (April—September) has been calculated. For example, for the Jhelum at Kohala, preceding season precipitation at Muzafferabad (October—March) provides the best correlation coefficient with both April—June (0.75) and April—September discharge (0.73), whereas summer discharge is best predicted by preceding precipitation at Astore (0.66).

Astore and Srinagar provide the best correlation coefficients despite the fact that the former is outside the catchment boundary. They may give a better representation of precipitation on the Greater Himalaya from which most runoff appears to originate. Muzafferabad was better in a few cases mainly with respect to the spring period and for stations at lower elevation. Neither Balakot nor Murree provided the best relationship for any period or catchment. Significant correlations were obtained, showing the potential for use in forecasting.

For the upper River Kunhar at Naran, forecasting of spring runoff is poor but, since the amount of spring runoff is small, this is not critical for whole season (April—September) forecasting. Relationships for spring months are much better for the lower Kunhar at Garhi Habibullah where there is a much greater volume of spring runoff. There is no significant correlation between concurrent precipitation and runoff during April—June for the Kunhar and Neelum but there are suggestions of correlation for the Jhelum, especially in lower reaches where spring melt is early. The addition of spring precipitation to winter precipitation sometimes results in improvements in relationships with April—September and July—September runoff.

Correlations are generally poor for the Poonch at Kotli, with weak but significant links to concurrent rainfall in the pre-monsoon period (April—June, $r = 0.49$) and, again, during the monsoon (July—September, $r = 0.53$). Surprisingly, the correlation coefficient is better for the monsoon period with Astore than with stations further south. Mangla is the only other summer flow record to be significantly correlated with summer rainfall.

In spite of the generally assumed relationship with temperature, as an index of energy input to snowmelt, only weak correlations were found between concurrent temperature and seasonal runoff (Table 3). With the exception of

Table 2 Best correlation coefficients between seasonal precipitation and seasonal runoff

River	Station	Forecast discharge for:						
	Based on Rainfall	April—September	April—September	April—September	April—September	July—September		
		October—March	April—June	October—March	October—June	October—March	October—June	July—September
Kunhar	Naran	Ast 0.17	Ast 0.30	Ast **0.76**	Ast **0.76**	Ast **0.65**	Ast **0.70**	Ast −0.27
Kunhar	Garhi Habibullah	Ast **0.67**	Sri *−0.45*	Ast **0.79**	Ast **0.73**	Sri **0.73**	Sri **0.71**	Sri 0.39
Neelum	Muzafferabad	Muz **0.56**	Ast 0.14	Ast **0.64**	Sri **0.58**	Sri **0.60**	Sri **0.73**	Sri 0.32
Jhelum	Chinari	Sri **0.75**	Sri *0.44*	Sri **0.66**	Sri **0.80**	Ast **0.54**	Sri **0.70**	Ast 0.17
Jhelum	Kohala	Muz **0.73**	Sri 0.26	Muz **0.73**	Muz **0.69**	Ast **0.66**	Muz **0.57**	Ast 0.06
Jhelum	Azad Pattan	Muz **0.75**	Muz *0.48*	Muz **0.75**	Ast **0.76**	Ast **0.75**	Ast **0.72**	Sri 0.19
Poonch	Kotli	Sri *0.38*	Sri **0.49**	Sri 0.29	Sri 0.36	Sri 0.18	Sri 0.20	Ast **0.53**
Kanshi	Palote	Muz 0.07	Muz 0.37	Sri 0.25	Sri 0.28	Sri 0.25	Sri 0.29	Ast *0.49*
Jhelum	Mangla 1960—1999			Ast **0.70**	Sri **0.78**			
Jhelum	Mangla 1920—1959	Sri **0.64**	Sri *0.37*	Sri **0.58**	Sri **0.66**	Sri *0.37*	Sri **0.47**	Sri **0.58**

Bold figures: significance 0.01; Italic: significance 0.05.
Ast: Astore; Sri: Srinagar; Muz: Muzafferabad.
The first line shows the station for which the best r value was obtained and the second line the correlation coefficient (r).

Table 3 Best correlation coefficients between seasonal temperature and seasonal runoff

River	Station	Forecast discharge for:						
		April–June		April–September		July–September		
	Based on temperature	January–March	April–June	January–March	April–September	January–March	January–June	July–September
Kunhar	Naran	Ast 0.06	Sri **0.57**	Ast −0.36	Ast −0.28	Ast *−0.41*	Sri **−0.79**	Sri −0.38
Kunhar	Garhi Habibullah	Ast −0.21	Sri 0.33	Ast *−0.45*	Ast −0.27	Ast **−0.58**	Ast **−0.68**	Sri −0.32
Neelum	Muzafferabad	Ast −0.18	Ast −0.26	Ast −0.32	Ast *−0.44*	Ast −0.35	Ast **−0.70**	Sri −0.32
Jhelum	Chinari	Ast **−0.61**	Ast *−0.47*	Ast **−0.66**	Ast *−0.40*	Ast **−0.61**	Ast **−0.65**	Ast −0.16
Jhelum	Kohala	Ast **−0.53**	Ast *−0.44*	Ast **−0.63**	Ast *−0.40*	Ast **−0.70**	Ast **−0.81**	Sri −0.28
Jhelum	Azad Pattan	Ast −0.36	Sri *−0.48*	Ast *−0.57*	Sri *−0.53*	Ast **−0.63**	Ast **−0.75**	Sri −0.30
Poonch	Kotli	Ast *−0.39*	Sri *−0.43*	Ast −0.06	Sri −0.19	Ast 0.03	Ast 0.15	Ast 0.10
Kanshi	Palote	Ast 0.24	Sri −0.29	Ast −0.11	Sri −0.08	Sri −0.08	Ast −0.20	Ast −0.13
Jhelum	Mangla 1960–1999			Ast **−0.61**	Ast *−0.34*			
Jhelum	Mangla 1920–1959	Sri −0.29	Sri −0.29	Sri *−0.36*	Sri **−0.44**		Sri **−0.41**	Sri −0.14

The first line shows the station for which the best *r* value was obtained and the second line the correlation coefficient (*r*).
Ast: Astore; Sri: Srinagar.
Bold figures: significance 0.01; Italic: significance 0.05.
Ast: Astore; Sri: Srinagar.

the Kunhar for the April—June period the correlations were negative. The absence of significant correlation between concurrent temperature and runoff suggests that glacier-melt as opposed to seasonal snow melt makes a limited contribution to basin runoff. In contrast, high correlation between concurrent temperature and summer runoff is a characteristic of high altitude glaciated basins of the Upper Indus such as the Hunza and Shyok (Archer, 2003). However, a surprising and consistent result is that significant negative correlation is achieved between runoff and temperature for the months preceding the target forecast runoff. This is particularly notable for July—September runoff.

Negative relationships between runoff and concurrent and prior seasonal average temperature have also been observed for neighbouring snow-fed catchments in the Indus basin (Archer, 2003). With respect to concurrent temperatures, Singh and Bengtsson (2005) suggest that increased temperature results in increased evaporative loss and, since snow cover volume is limiting, reduced runoff; estimating reductions of ~18% for a 2 °C rise in temperature. A physical explanation for the negative relationship between runoff and preceding temperature is more uncertain. However, Schär et al. (2004) suggest that runoff may also be sensitive to fluctuations in mean monthly temperature, T, in the transition periods to/from freezing temperatures, October—November and March—April. This may have an influence on whether the precipitation is solid or liquid and thus whether the runoff is instantaneous or delayed. Irrespective of the physical explanation, the high correlations obtained with both winter rainfall and concurrent and preceding temperatures suggests potential for practical use in operational forecasting.

Seasonal flow forecasting for Mangla dam

The significant positive relationships established between climatic variables and flow, and the broad spatial correlation of these climatic variables, opens up the possibility of a variety of strategies for flow forecasting. A limited number of these strategies are tested here by using a lumped approach for the Jhelum at Kohala and the Poonch at Kotli which together represent 85% of the catchment area to Mangla. Kohala (1965—1996) is preferred to Azad Patan (1978—1996) because of the longer flow record.

For the purposes of illustration the analysis has been restricted to seasonal forecasting at the end of March for the seasonal periods April—June, April—September and July—September. It is considered more operationally effective to use the Astore and Muzafferabad climate records (rather than Srinagar) for flow forecasting, since they are under the control of the Pakistani authorities.

Seasonal flow forecasts are produced using a split-sample approach by fitting a stepwise multiple regression relationship to part of the data (1965—1979) and using an independent period for model validation (1979—1996). Due to extraordinary high monsoon rainfall in 1976 affecting summer flows at Kotli (flows were five times the mean and seven times the median flows), and to a certain extent at Kohala, this year has been omitted from the analysis. The correlation analysis suggests that winter half-year rainfall (October—March), winter rainfall (January—March) and winter temperature (January—March) are the most likely explanatory variables for flow prediction during the spring and summer. However, a more flexible fitting scheme, a stepwise 2-way algorithm, is used to determine the optimal multiple linear regression model for seasonal average flow, Q in Kohala + Kotli for April—June, April—September and July—September (notation based on Schär et al., 2004):

$$Q_t = \phi^0 + \sum_s \phi_s^P P_{t,s} + \sum_s \phi_s^T T_{t,s} + \sum_s \phi_s^Q Q_{t,s} \quad (1)$$

Here, the variable P represents precipitation amount (in millimetres) at Astore or Muzzaferabad accumulated over the periods under consideration; Q represents the average flow (in $m^3\,s^{-1}$) at Kohala + Kotli over the periods under consideration; T represents average temperature (in °C) at Astore over the periods under consideration; the subscripts t and s, respectively denote the year and season (where periods of 3—6 months are considered). The algorithm works by introducing explanatory variables that are significant at the α-level = 0.15 (i.e. p = 15%) to the statistical model. If any explanatory variable becomes less than α-level = 0.15 then it is eliminated from the model. The remaining coefficients φ are recomputed after each addition or elimination. The p-value for each explanatory variable is based on a t-test that verifies whether the variable can be added to or eliminated from the regression model (i.e. $\varphi = 0$ as null hypothesis).

The resulting statistical estimates for April—June, July—September and April—September runoff, $\hat{Q}_{AMJ}$, $\hat{Q}_{JAS}$, and $\hat{Q}_{AMJJAS}$, respectively, are shown in Eqs. (2)—(4) below. All precipitation variables refer to recorded data at Muzzaferabad and all temperature variables refer to recorded data at Astore.

$$\hat{Q}_{AMJ} = 652.9 + 1.66P_{t,DJFM} + 1.78Q_{t,JFM} - 1.6P_{t,ONDJ} - 97T_{t,DJFM} \quad (2)$$

$$\hat{Q}_{JAS} = 420.2 + 3.09P_{t,JFM} \quad (3)$$

$$\hat{Q}_{AMJJAS} = 1027 + 1.79P_{t,DJFM} - 106T_{t,JFM} - 1.06P_{t,ONDJ} \quad (4)$$

where $P_{t,ONDJ}$ refers to the accumulated precipitation (in mm) from October to January, $P_{t,DJFM}$ refers to the accumulated precipitation (in mm) from December to March, $P_{t,JFM}$ refers to the accumulated precipitation (in mm) from January to March, $T_{t,DJFM}$ refers to the mean temperature (in °C) during the months from December to March, $T_{t,JFM}$ refers to the mean temperature (in °C) during the months from January to March and $Q_{t,JFM}$ refers to the average flow (in $m^3 s^{-1}$) from January to March.

In the model, these climate variables are able to explain r^2 = 70.6%, 40.9% and 83.1% of the variability in average flow from April—June, July—September and April—September, respectively during the calibration period from 1965 to 1979 (excluding 1976). The p-values and confidence intervals associated with each explanatory variable in each model can be found in Table 4.

Within all the flow prediction equations, precipitation from either December or January to March is a significant explanatory variable ($p < 0.05$). This suggests that winter precipitation provides the primary source for summer runoff. It remains unclear why precipitation from October to January is a significant explanatory variable for summer season (April—September) flow. Serial correlation with average flow for January to March also provides a significant

Table 4 Summary statistics for regression models: *p*-values and confidence intervals for explanatory variables

Flow model	Explanatory variable	*p*-Value	Upper 95% confidence interval	Lower 95% confidence interval
$\hat{Q}_{AMJ}$	ϕ	0.001	1009.03	296.77
	$P_{t,DJFM}$	0.000	2.69	0.63
	$Q_{t,JFM}$	0.009	2.98	0.58
	$P_{t,ONDJ}$	0.034	−0.23	−2.97
	$T_{t,DJFM}$	0.098	4.08	−198.08
$\hat{Q}_{JAS}$	ϕ	0.248	1098.75	−258.35
	$P_{t,JFM}$	0.014	5.19	0.99
$\hat{Q}_{AMJJAS}$	ϕ	0.000	1336.09	717.91
	$P_{t,DJFM}$	0.000	2.63	0.93
	$T_{t,JFM}$	0.059	−1.65	−210.35
	$P_{t,ONDJ}$	0.094	0.13	−2.25

predictor of spring (April—June) flow. Winter temperature from December or January to March also has a significant influence on spring and summer season (April—September) flow. This may be a result of sensitivity to fluctuations in mean monthly temperature in the transition period from freezing temperatures to spring melt in March—April or that temperature during these months, when the majority of winter precipitation falls, control the elevation at which precipitation falls as snow or rain. Therefore, lower temperatures may mean a greater accumulation of snowfall that can be melted in the summer months.

Using the multiple linear regression relationships derived above, forecasts of seasonal average flows into Mangla were made for both the model calibration period from 1965 to 1979 and an independent validation period from 1980 to 1991. Fig. 4 shows time series of observed and fitted average seasonal flow for Kohala + Kotli into Mangla for the model calibration period from 1965 to 1979 and observed and predicted average seasonal flow for the 1980 to 1991 forecast period — panels (a—c) show the April—June, July—September and April—September flows, respectively. Comparison of the observed and predicted flows shows that, using valley station based estimates of precipitation and temperature, the statistical models are able to capture most of the observed inter-annual variability in flows over the calibration period from 1965 to 1979 even without explicit treatment of the snowmelt-runoff process such as through the use of a physically-based model.

The forecast models for April—June and April—September flows are able to successfully predict flow within 15% of observed flows for 83% and 92% of the years of the model validation period from 1979 to 1991 (excluding 1976) and explain r^2 = 58% and r^2 = 60% of the variability, respectively. The forecast model for July—September flows is poorer, being able to predict flows within 20% of observed flows for only 66% of the years and having an explained variance of only r^2 = 12%.

Using a ROC (relative operating characteristic) scores test (Mason, 1982; Mason and Graham, 1999), a method of representing forecast skill that is based on a simple 2×2 contingency table, we can determine whether each model can be accurately used for forecasting. The ROC score is based on whether a pre-defined event can be warned against successfully; here defined as whether we can forecast above-average seasonal flows for Kohala + Kotli into Mangla (>1595, 1460 and 1528 $m^3 s^{-1}$, respectively for April—June, July—September and April—September average flows over 1965—1991, see Fig. 4). A series of forecasts of above-average ($> \bar{Q}_t$) and below-average ($< \bar{Q}_t$) flow using the forecast models for the calibration period 1965—1979 and the validation period 1980—1991 is compared with the observed flow series (see Tables 5—7). Note that years where both observed and predicted flow are within 5% of the observed average flow are omitted from the analysis to allow for slight under- and over-prediction by the models near to the average (these are marked with bold triangles in Fig. 4). The ROC score compares hit and false alarm rates, which respectively indicate the proportion of times a correct forecast is provided, and the proportion of times a forecast is incorrect. The expected ROC score from random chance is 0.5. If the ROC score is greater than 0.5 there is evidence of skill. ROC scores, hit rates and false alarm rates for all three models are summarised in Table 8.

The ROC score is obtained by calculating the area under the ROC curve. A ROC curve provides a graphical representation of the relationship between the hit and false alarm prediction rates of a model. The *y*-axis measures the sensitivity of the model or hit rate and is calculated as

$$y = \frac{H}{H + M} \tag{5}$$

where *H* is the number of correct forecasts (hits or true positives) and *M* is the number of incorrect negative forecasts (misses or false negatives).

The *x*-axis measures the specificity of the model or the ability of the model to identify true negatives by using an equation that gives the false alarm rate:

$$x = 1 - \frac{CR}{CR + FA} \tag{6}$$

where CR is the number of correct rejections (true negatives) and FA is the number of false alarms (false positives).

The area under the curve (the ROC Score) is then calculated using the trapezoidal rule as

$$ROC = \int f(x)dx\left[\frac{x_{i+1} + x_i}{2}\right](y_{i+1} + y_i) \tag{7}$$

Table 5 shows that using the Apr-Sep forecast model we predict above-average flows for 4 years during the model calibration period from 1965 to 1979 (including 1976), with four correct forecasts (hits) and no incorrect forecasts (false

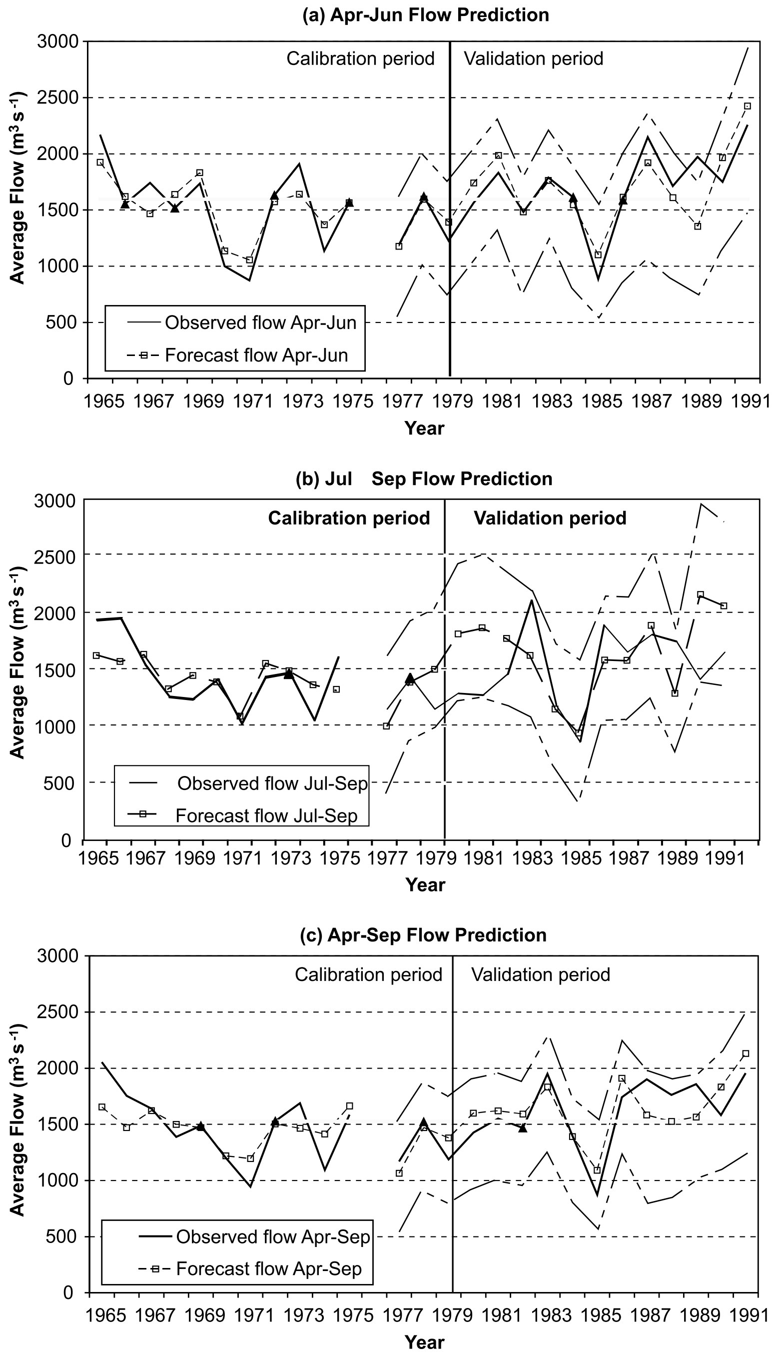

Figure 4 Time series of observed and predicted seasonal runoff for Kohala + Kotli inflows into Mangla for: (a) April—June, (b) July—September, and (c) April—September, for the calibration period, 1965—1979 (excluding 1976), and the validation period, 1980—1991. The 95% prediction intervals are shown in each case for the validation period.

alarms). Similarly, we predict below-average flows for 8 years, with six correct forecasts (correct rejections) and two incorrect forecasts (misses). This suggests a hit rate of 0.67, and a false alarm rate of 0.0, with a ROC score of 0.83. During the model validation period from 1980 to 1991, the model performs well, predicting above-average flows for 8 years, with seven hits and one false alarm. Below-average flows are predicted for 3 years, with two correct rejections and only one miss. This gives a hit rate of 0.88, a false alarm rate of 0.33 and a ROC score of 0.77. This implies that the model provides good skill in forecasting above-average April—September flows for Kohala + Kotli into Mangla.

The results for the April—June forecasts are comparable (Table 6) with predictions of above-average flows for 4 years during the model calibration period from 1965 to 1979 (including 1976), giving three hits and one false alarm (1976). For below-average flows, there were five correct rejections and one miss. This suggests a hit rate of 0.75, a false alarm rate of 0.17, and a ROC score of 0.79. During

Table 5 Contingency table for the forecast of above-average April—September flow ($> \bar{Q}_{AMJJAS}$ excluding flows within 5% of observed average) into Mangla, for (a) the model fitting period 1965—1979 (excluding 1976) and (b) the forecast period 1980—1991

Event observed ($> \bar{Q}_{AMJJAS}$)?	Yes	No
(a)	Event forecast ($> \bar{Q}_{AMJJAS}$)?	
Yes	4 (0.33)	2 (0.17)
No	0 (0.00)	6 (0.50)
(b)	Event forecast ($> \bar{Q}_{AMJJAS}$)?	
Yes	7 (0.64)	1 (0.09)
No	1 (0.09)	2 (0.18)

Indicating the relative fraction of hits (forecast YES, observed YES), misses (forecast NO, observed YES), false alarms (forecast YES, observed NO), and correct rejections (forecast NO, observed NO). Note that a YES forecast indicates a forecast of above-average runoff and a NO forecast indicates a forecast of below-average runoff.

Table 6 Contingency table for the forecast of above-average April—June flow ($> \bar{Q}_{AMJ}$, excluding flows within 5% of observed average) into Mangla, for (a) the model fitting period 1965—1979 (excluding 1976) and (b) the forecast period 1980—1991

Event observed ($> \bar{Q}_{AMJ}$)?	Yes	No
(a)	Event forecast ($> \bar{Q}_{AMJ}$)?	
Yes	3 (0.30)	1 (0.10)
No	1 (0.10)	5 (0.50)
(b)	Event forecast ($> \bar{Q}_{AMJ}$)?	
Event observed ($> \bar{Q}_{AMJ}$)?	Yes	No
Yes	6 (0.67)	1 (0.11)
No	1 (0.00)	2 (0.22)

Details are the same as for Table 5.

the forecast period from 1980 to 1991 the model performs even better, with predictions of above-average flows for 6 years, giving six hits and no false alarms. The model predicts below-average flows for 3 years with two correct rejections and one miss. This produces a hit rate of 0.86, a false alarm rate of 0.0 and a ROC score of 0.93. This suggests that the model provides excellent predictions of above-average April—June flows into Mangla.

The results for the July—September forecast (Table 7) are poorer. We predict above-average runoff for 6 years during the model calibration period (including 1976), with

Table 7 Contingency table for the forecast of above-average July—September flow ($> \bar{R}_{JAS}$, excluding flows within 5% of observed average) into Mangla, for (a) the model fitting period 1965—1979 (excluding 1976) and (b) the forecast period 1980—1991

Event observed ($> \bar{Q}_{JAS}$)?	Yes	No
(a)	Event forecast ($> \bar{Q}_{JAS}$)?	
Yes	4 (0.31)	1 (0.08)
No	2 (0.15)	6 (0.46)
(b)	Event forecast ($> \bar{Q}_{JAS}$)?	
Event observed ($> \bar{Q}_{JAS}$)?	Yes	No
Yes	5 (0.42)	1 (0.08)
No	4 (0.33)	2 (0.17)

Details are the same as for Table 5.

four hits and two false alarms. For below-average runoff, there were six correct rejections and one miss. This suggests a hit rate of 0.80, a false alarm rate of 0.25, and a ROC score of 0.77. However, for the forecast period the model performs more poorly, predicting above-average runoff for 9 years, with five hits and four false alarms. For below-average runoff, there were two correct rejections and one miss. This suggests a hit rate of 0.83 but a high false alarm rate of 0.67, producing a ROC score of only 0.58. This ROC score suggests that only poor forecasts may be obtained for summer runoff; possibly due to the influence of concurrent monsoonal rainfall and concurrent summer temperatures on melting rates.

Discussion and conclusions

The analysis demonstrates that despite catchment size and complexity, forecasts of summer flows of sufficient reliability to provide a useful basis for practical water management can be achieved for the Jhelum basin. A multiple linear regression model using seasonal temperature predictors at Astore and precipitation predictors at Muzzaferabad was able to successfully forecast summer season flows for Kohala + Kotli into Mangla to within 15% of observed values for 92% of years. Forecasts for April—September and April—June runoff, respectively gave ROC scores of 0.77 and 0.93 — suggesting that they provide good forecasting ability for summer season flows and excellent forecasting ability for spring flows in this region. However, for the true summer runoff from July to September, only poor forecasts were obtained with a ROC score of 0.58. This may be due to the influence of monsoonal rainfall and the impacts of concurrent temperature on snowmelt rates contributing to July—September flows in the Jhelum River. However, using predictors up to March gives a lead time of 1 month for spring flow planning requirements and 3 months for summer planning requirements; vital for the management of water

Table 8 Summary of ROC scores, hit rates and false alarm rates for all seasonal forecasting models for calibration and validation periods

Flow model	Time period	Hit rate	False alarm rate	ROC score
$\hat{Q}_{AMJ}$	Calibration (1965–1979)	0.75	0.17	0.79
	Validation (1980–1991)	0.86	0.00	0.93
$\hat{Q}_{JAS}$	Calibration (1965–1979)	0.80	0.25	0.77
	Validation (1980–1991)	0.83	0.67	0.58
$\hat{Q}_{AMJJAS}$	Calibration (1965–1979)	0.67	0.00	0.83
	Validation (1980–1991)	0.88	0.33	0.77

resources utilisation and hydropower production across the region.

Although this study provides useful regression models for the forecasting of summer season flows for Kohala + Kotli into Mangla using scarce data from valley stations, it is believed that improved seasonal forecasts may still be achieved by the use of:

1. A regression based distributed approach in which contributions from sub-catchments are considered separately to take advantage of the different dominant climatic controls on different catchments.
2. More sophisticated modelling techniques such as physically-based models or artificial neural network models. These provide a huge potential for the simulation of the non-linear behaviour of hydrological systems and it may be advantageous to use a distributed hydrological model rather than the statistical approach used here.
3. A wider range of climate, GIS elevation and snow cover data. Work in neighbouring areas of Central Asia (Schär et al., 2004) has found that reanalysis data such as ERA-15 is useful for forecasting. Further work will assess the utility of the more recently available ERA-40 dataset for the forecasting of seasonal runoff in the Karakoram region. This is available from ECMWF and covers the 1957–2001 period (with possible extensions into the future). The use of a spatial dataset rather than the point data used in this study may increase the predictive power of the statistical model. Further improvements in seasonal runoff forecasting in the region may be provided by the development of accurate forecasting methods for seasonal temperature using teleconnections such as the El Niño Southern Oscillation. Additional datasets to represent the Central Asian precipitation climate based on direct observations and the output of a regional climate model (Schiemann et al 2008) also deserve further study.
4. Application of remote forcings to improve streamflow prediction accuracy and lead time. Significant effects of the North Atlantic Oscillation (NAO) and El Niño Southern Oscillation (ENSO) on winter precipitation have been demonstrated for Central South West Asia (Syed et al., 2006) and more specifically for the upper Indus basin (Archer and Fowler, 2004; Fowler and Archer, 2006).

The use of such teleconnections in improving seasonal streamflow forecasting skill requires further investigation.

The use of a simple regression model based on observed surface precipitation and temperature for forecasting seasonal runoff can be considered a standard against which improvements using such more sophisticated approaches can be judged.

In conclusion, irrigated agriculture constitutes the largest sector of Pakistan's economy, accounting for half the employed labour force and the largest source of foreign exchange income. Even small changes to the planning and management of water releases from Mangla based on improved forecast information could confer significant economic benefits to the region. The future growth of population and associated land and water scarcity may place additional demands on water management and forecasts may also become more critical with climate change. The seasonal forecasting of flows through simple methods, such as those outlined in this paper, may thus become a fundamental requirement for the successful management of water in the region.

Acknowledgments

The work was initiated whilst the first author was a volunteer with Voluntary Service Overseas (VSO) and employed by the German Agency for Technical Development (GTZ). The authors wish to thank colleagues of both agencies for the opportunity and their support. Support was also provided by officials of WAPDA and at the Pakistan Meteorological Department. Dr. Hayley Fowler was supported by a NERC fellowship award (NE/D009588/1). The authors would also like to thank two anonymous reviewers whose comments helped to improve the paper.

References

Archer, D.R., 2003. Contrasting hydrological regimes in the upper Indus Basin. Journal of Hydrology 274, 198–210.

Archer, D.R., 2004. Hydrological implications of spatial and altitudinal variation in temperature in the upper Indus basin. Nordic Hydrology 35 (3), 213–227.

Archer, D.R., Fowler, H.J., 2004. Spatial and temporal variations in precipitation in the Upper Indus Basin, global teleconnections and hydrological implications. Hydrology and Earth System Sciences 8, 47–61.

Asianics Agro-Dev International (Pvt) Ltd., 2000. Tarbela Dam and related aspects of the Indus Basin Pakistan. A WCD case study prepared as an input to the World Commission on Dams, Capetown. <http://www.dams.org>.

Barlow, M., Cullen, H., Lyon, B., 2002. Drought in central and southwest Asia: La Niña, the warm pool, and Indian Ocean precipitation. Journal of Climate 15, 697–700.

Barlow, M., Wheeler, M., Lyon, B., Cullen, H., 2005. Modulation of daily precipitation over southwest Asia by the Madden—Julian oscillation. Monthly Weather Review 133, 3579—3594.

Binnie, G.M., Mansell-Moulin, M., 1966. The estimated probable maximum storm and flood on the Jhelum River — a tributary of the Indus. In: River Flood Hydrology, Proceedings of a Symposium of the Institution of Civil Engineers, March 1965. ICE, London, pp. 89—211.

Binnie, G.M., Gerrard, R.T., Eldridge, J.G., Kirmani, S.S., Davis, C.V., Dickenson, J.C., Gwyther, J.R., Thomas, A.R., Little, A.L., Clark, J.F.F., Seddon, B.T., 1967. Engineering of Mangla. Proceedings of Institution Civil Engineers 38, 345—544.

Carroll, T.R., 1995. GIS used to derive operational hydrologic products from in situ and remotely sensed data. In: Carrera, A., Guzzetti, F. (Eds.), Geographical Information Systems in Assessing Natural Hazards. Kluwer Academic Publishing, Netherlands, pp. 335—342.

Clark, M.P., Hay, L.E., McCabe, G.J., Leavsey, G.H., Serreze, M.C., Wilby, R.L., 2003. Use of weather and climate information in forecasting water supply in the Western United States. In: LewisJr, W.M. (Ed.), Water and Climate in the Western United States. University Press of Colorado, pp. 9—92 (Chapter 5).

Day, G.N., 1985. Extended streamflow forecasting using NWSRFS. Journal of Water Resources Planning and Management 111, 157—170.

Dey, B., Goswami, D.C., Rango, A., 1983. Utilization of satellite snow-cover observations for seasonal streamflow estimates in the Western Himalayas. Nordic Hydrology 14, 257—266.

De Scally, F.A., 1994. Relative importance of snow accumulation and monsoon rainfall data for estimating annual runoff, Jhelum basin, Pakistan. Hydrological Sciences Journal 39 (3), 199—216.

Farnes, P.E., 1985. Predicting time of peak snowmelt runoff from snow pillow runoff. In: Proceedings of the Western Snow Conference 52, pp. 132—138.

Fowler, H.J., Archer, D.R., 2005. Hydro-climatological variability in the Upper Indus Basin and implications for water resources. In: Wagener, T. et al. (Eds.), Regional Hydrological Impacts of Climatic Change — Impact Assessment and Decision Making, vol. 295. IAHS Publication, pp. 131—138.

Fowler, H.J., Archer, D.R., 2006. Conflicting signals of climatic change in the Upper Indus Basin. Journal of Climate 19 (17), 4276—4293.

Garstka, W.U., 1964. Snow and Snow Survey. In: Chow, V.T. (Ed.), Handbook of Applied Hydrology. McGraw-Hill, New York.

Gibson, J.K., Kallberg, P., Uppala, S., Hernandez, A., Nomura, A., Serrano, A., 1999. ERA description, Version 2. ERA-15 Project Report Series 1, ECMWF, Reading, United Kingdom, p. 74.

Hall, D.K., Martinec, J., 1985. The Remote Sensing of Snow and Ice. Chapman and Hall, London.

Hewitt, K., 2005. The Karakoram anomaly? Glacier expansion and the 'elevation effect', Karakoram Himalaya. Mountain Research and Development 25 (4), 332—340.

Hoerling, M., Kumar, A., 2003. The perfect ocean for drought. Science 299, 691—694.

Khan, A.R., Ullah, K.K., Muhammad, S., 2002. Water availability and some macro level issues related to water resources planning and management in the Indus Basin Irrigation System in Pakistan. <http://www.riob.org/ag2000/pakistan.htm>.

Kolb, H., 1992. Abflussverhalten von Flüssen in Hochgebirgen Nordpakistans (runoff characteristics of rivers in high mountainous areas of northern Pakistan). Beitrage und Materialen zur Regionalen Geographie H7, 21—102.

Makhdoom, M.T.A., Solomon, S.I., 1986. Attempting flow forecasts of the Indus River, Pakistan using remotely sensed snow-cover data. Nordic Hydrology 17, 171—184.

Mariotti, A., Ballabrera-Poy, J., Zeng, N., 2005. Tropical influence on Euro-Asian autumn rainfall variability. Climate Dynamics 24, 511—521.

Mason, I., 1982. A model for the assessment of weather forecasts. Australian Meteorological Magazine 30, 291—303.

Mason, S.J., Goddard, L., 2001. Probabilistic precipitation anomalies associated with ENSO. Bulletin of the American Meteorological Society 82, 619—638.

Mason, S.J., Graham, N.E., 1999. Conditional probabilities, relative operating characteristics, and relative operating levels. Weather Forecasting 14, 713—725.

Popov, E.G., 1972. Snowmelt runoff forecasts; theoretical problems. In: UNESCO/WMO/IAHS Symposia on the Role of Snow and Ice in Hydrology, vol. 107. IAHS Publication, Banff, pp. 829—839.

Quick, M.C., 1972. Forecasting runoff operational practices. In: UNESCO/WMO/IAHS Symposia on the Role of Snow and Ice in Hydrology, vol. 107. IAHS Publication, Banff, pp. 943—955.

Rango, A., Salomonson, V.V., Foster, J.L., 1977. Seasonal streamflow estimation in the Himalayan region employing meteorological satellite snow-cover observations. Water Resources Research 13, 109—112.

Rodwell, M.J., Hoskins, B.J., 1996. Monsoons and the dynamics of deserts. Quarterly Journal of the Royal Meteorological Society 122, 1385—1404.

Schär, C., Vasilina, L., Pertziger, F., Dirren, S., 2004. Seasonal runoff forecasting using model-assimilated precipitation data. Journal of Hydrometeorology 5 (5), 959—973.

Schiemann, R., Glazirina, M.G., Schär, C., 2007. On the relationship between the Indian summer monsoon and river flow in the Aral Sea basin. Geophysical Research Letters 34, L05706. doi: 10.1029/2006GL028926.

Schiemann, R., Lüthi, D., Vidale, P.L., Schär, C., 2008. The precipitation climate of central Asia — intercomparison of observational and numerical data sources in a remote semiarid region. International Journal of Climatology 28, 295—314.

Singh, P., Bengtsson, L., 2005. Impact of warmer climate on melt and evaporation for the rainfed, snowfed and glacierfed basins in the Himalayan region. Journal of Hydrology 300, 140—154.

Syed, F.S., Giorgi, F., Pal, J.S., King, M.P., 2006. Effect of remote forcings on the winter precipitation of central southwest Asia part 1: observations. Theoretical and Applied Climatology 86, 147—160. doi: 10.1007/s00704-005-0217-1.

Wedgbrow, C.S., Wilby, R.L., Fox, H.R., O'Hare, G., 2002. Prospect for seasonal forecasting of summer drought and low river flow anomalies in England and Wales. International Journal of Climatology 22, 219—236.

Wood, A.W., Maurer, E.P., Kumar, A., Lettenmaier, D.P. 2002. Long Range Experimental Hydrologic Forecasting for the Eastern US. Journal of Geophysical Research 107, D20, 4429. doi: 10.1029/2001JD000659.